Experimental studies of the $\Lambda(1405)$

physics654 – Seminar on exotic multi-quark states

Jakob Krause

krause@hiskp.uni-bonn.de | krausejm

Tutor: Georg Scheluchin

scheluchin@physik.uni-bonn.de

18.06.2021

Motivation

What is special about the $\Lambda(1405)$?

- mass does not fit well into constituent quark models
- invariant mass distribution (line shape) differs significantly from usual Breit-Wigner shape
- candidate for an exotic multiquark state (bound system of $\overline{K}N$) since its mass lies just below production threshold

there are many different theoretical approaches to explain this behavior
$\rightarrow$ need for more experimental data!

Table of contents

1. Experimental setup
2. Line-shape measurement
3. Spin-parity measurement
4. Conclusion

1. Experimental setup

2. Line-shape measurement

3. Spin-parity measurement

4. Conclusion

Continuous Electron Beam Accelerator Facility (CEBAF)

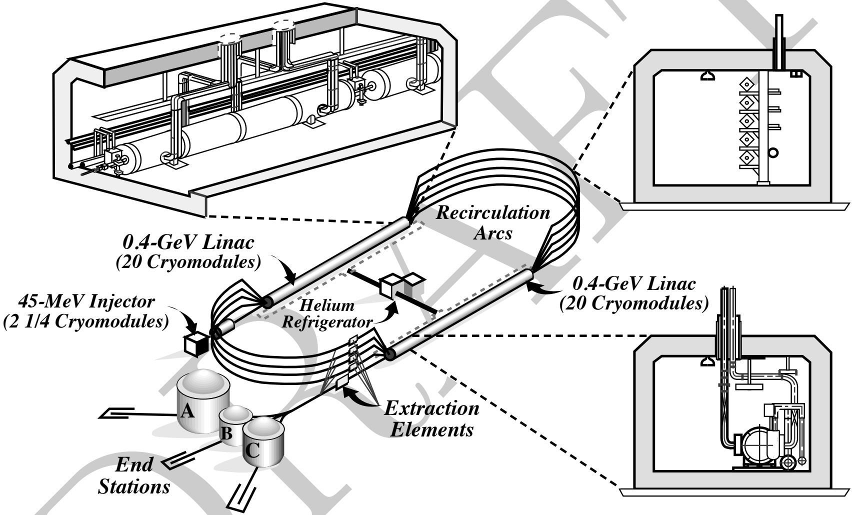

CEBAF layout at Jefferson Lab, [Mecking et al. 2003]

Continuous Electron Beam Accelerator Facility (CEBAF)

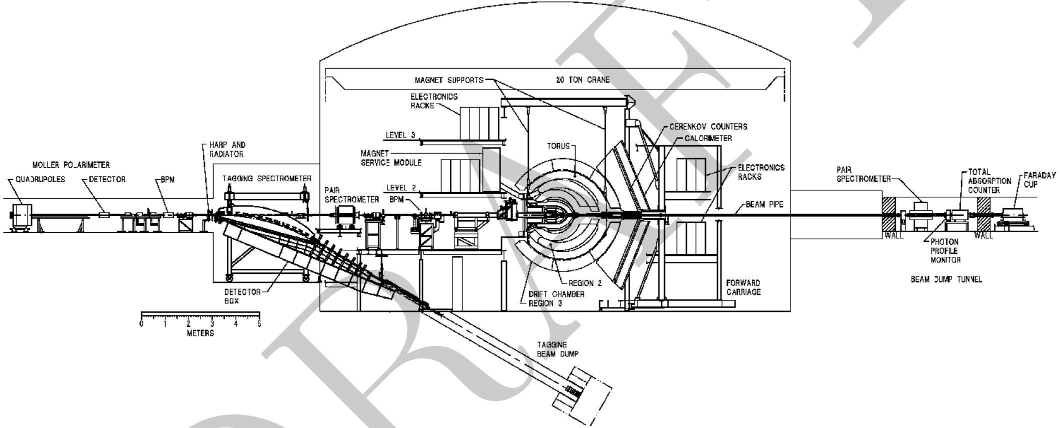

Figure 1: Overview of the CLAS detector setup, including the tagger, [Mecking et al. 2003]

CEBAF Large Acceptance Spectrometer (CLAS)

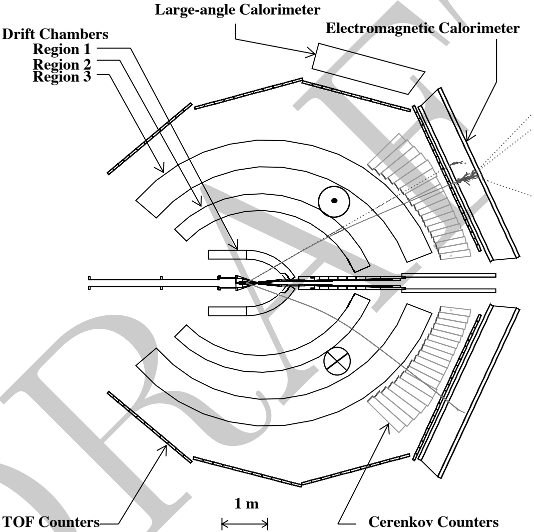

CLAS layout at Jefferson Lab, [Mecking et al. 2003]

1. Experimental setup

2. Line-shape measurement

3. Spin-parity measurement

4. Conclusion

Reaction kinematics

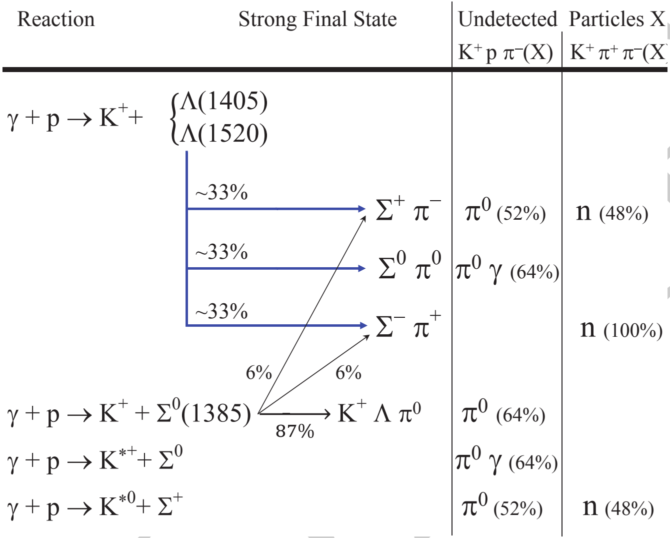

$\Sigma^+ \to p\pi^0$

$\Sigma^+ \to n\pi^+$

$\Sigma^0 \to \gamma\Lambda \quad \to \gamma p\pi^-$

$\Sigma^- \to n\pi^-$

$\Lambda \to p\pi^-$

Possible and studied reactions in the analysis of the lineshapes of $\Lambda(1405)$, [Moriya, Schumacher, Adhikari et al. 2013]

Event selection

two sets of reactions that the detector sees

1. $K^+ p \pi^- (X)$
2. $K^+ \pi^+ \pi^- (X)$

there are many cuts that can be made that apply to both

Initial selection of particles

- particle identification using TOF counters and momentum measurements
- kinematic cuts from Monte Carlo

Event selection – Particle identification

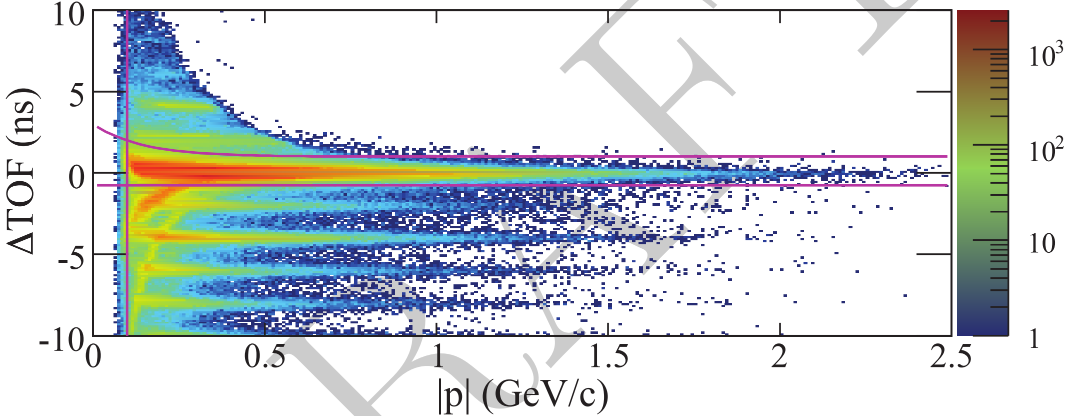

ΔTOF for π^+ @ $2.35 < W < 2.45\,\mathrm{GeV}$, applied cuts are shown in magenta. [Moriya, Schumacher, Adhikari et al. 2013]

Event selection

Binning of data

the data was divided:

- 10 bins in $W = \sqrt{s}$ dividing 2 GeV to 3 GeV in steps of 100 MeV
- 20 bins in $\cos\theta^{K^+}_{\mathrm{CMS}}$ dividing -1 to 1 in steps of 0.1

$\rightarrow$ the following analysis was performed independently in every bin of energy and angle!

Event selection

extracting $\Lambda\pi^0$ and $\Sigma^+\pi^-$

- reminder: $\Lambda \to p\pi^-, \Sigma^+ \to p\pi^0$
- final state particles: $K^+p\pi^-(\pi^0)$
- determine p_π via missing mass fit
- apply cuts based on fits to the invariant masses $M_{p\pi^-}$ and $M_{p\pi^0}$

extracting $\Sigma^+\pi^-$ and $\Sigma^-\pi^+$

- reminder: $\Sigma^\pm \to n\pi^\pm$
- final state particles: $K^+\pi^+\pi^-(n)$
- determine p_n via missing mass fit
- apply cuts based on fits to the invariant masses $M_{n\pi^\pm}$

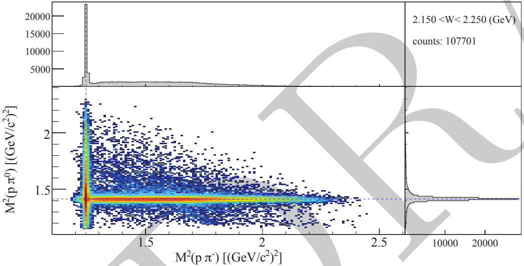

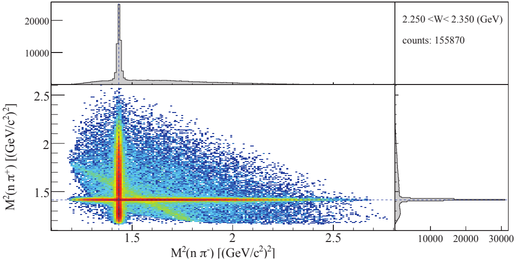

DALITZ-like plots of the above mentioned invariant masses, [Moriya, Schumacher, Adhikari et al. 2013]

Event selection

extracting $\Sigma^0\pi^0$

- reminder: $\Sigma^0 \to \gamma\Lambda \to \gamma p\pi^-$
- final state particles: $K^+p\pi^-(\gamma\pi^0)$ - missing mass fit is not applicable here: demand the missing mass is sufficiently greater than m_π
- make cuts based on the invariant mass $M_{p\pi^-}$
- now the missing mass ($\gamma p \to K^+X$) gives the $\Sigma^0\pi^0$ lineshape

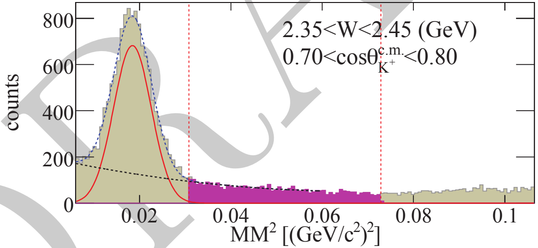

Missing mass of the reaction $\gamma p \to K^+p\pi^-(X)$, selection range in magenta. [Moriya, Schumacher, Adhikari et al. 2013]

Measurements and analysis

- now the signal regions have been established
- the true lineshape of the $\Lambda(1405)$ has to be extracted from the vast of reactions $\rightarrow$ any other contributions have to be substracted
- strategy: use of MONTE-CARLO fits to the data, simulating the contribution of other resonances using the PDG widths and masses

Measurements and analysis

some fit results:

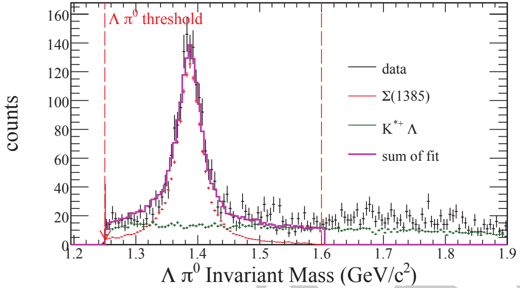

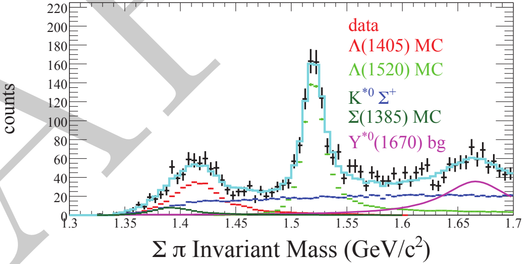

Sample fit results of invariant mass spectra for a single bin in energy and angle, [Moriya, Schumacher, Adhikari et al. 2013]

Interpretation of the results

having substracted all unwanted reactions, one can obtain the true $\Lambda(1405)$ lineshapes:

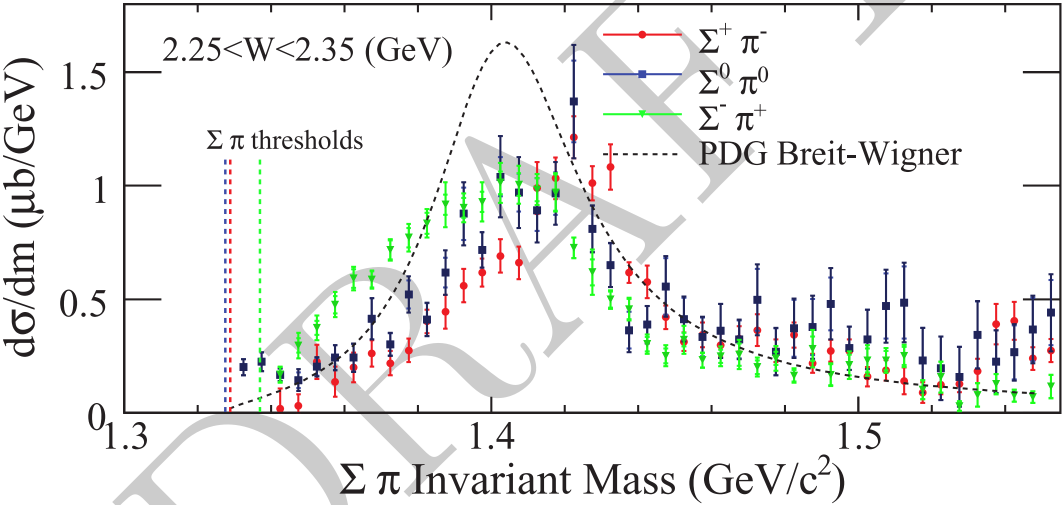

Lineshapes of the $\Lambda(1405)$ for the 3 different decay channels and the PDG Breit-Wigner. The data were summed over all angles for better statistics. [Moriya, Schumacher, Adhikari et al. 2013]

Interpretation of the results

there are in fact predictions of the lineshapes differing by decay channel [Nacher et al. 1999].
→ main idea: not one amplitude, but two due to isospin decomposition.

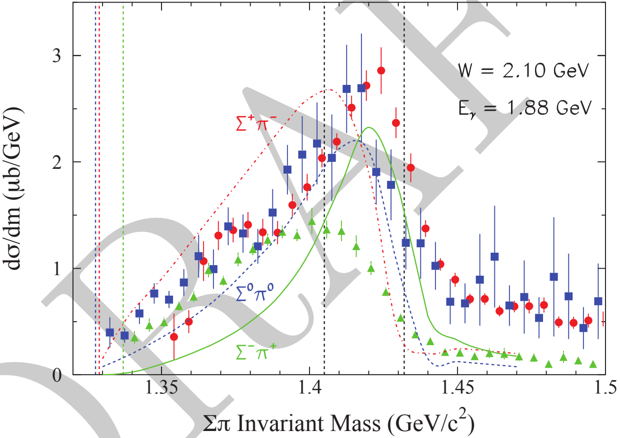

Lineshapes of the Λ(1405) for the 3 different decay channels and the prediction of [Nacher et al. 1999], [Moriya, Schumacher, Adhikari et al. 2013]

Interpretation of the results

MORIYA ET AL. saw two main reasons for the lineshapes differing from a simple BREIT-WIGNER:

1. isospin decomposition
2. channel coupling between the detected $\Sigma\pi$ and $N\overline{K}$ final states

Isospin decomposition

let

$$|t_I|^2 = |\langle I,0|T^{(I)}|\gamma p\rangle|^2,$$

then we can write (neglecting $I=2$ using CGK)

$$|T_{\pi^-\Sigma^+}|^2 = \frac{1}{3}|t_0|^2 + \frac{1}{2}|t_1|^2 - \frac{2}{\sqrt{6}}t_0 t_1 \cos\phi_{01}$$

$$|T_{\pi^0\Sigma^0}|^2 = \frac{1}{3}|t_0|^2$$

$$|T_{\pi^+\Sigma^-}|^2 = \frac{1}{3}|t_0|^2 + \frac{1}{2}|t_1|^2 + \frac{2}{\sqrt{6}}t_0 t_1 \cos\phi_{01}$$

Channel coupling

the t_I are described by one or two BREIT-WIGNER amplitudes with mass dependent widths Γ

$\rightarrow$ modify the amplitude preserving analyticity [Flatté 1976] including the $N\overline{K}$ decay channel available at threshold

$m_K + m_p \approx 1434\,\mathrm{MeV}$

Interpretation of results

fits with two $I = 1$ and one $I = 0$ amplitudes lead to best agreement with measured data

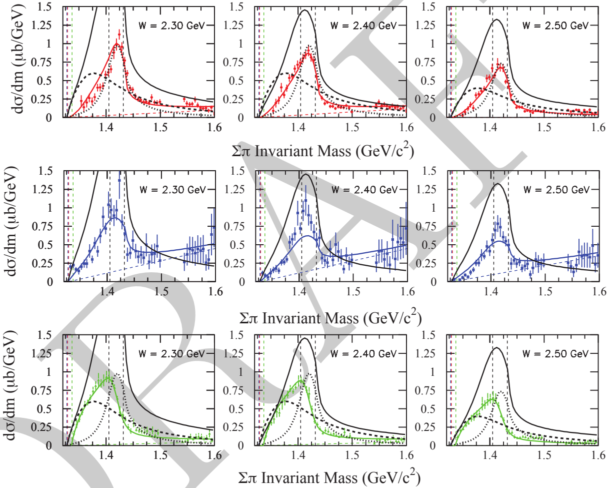

Data and fits for $\Sigma^a\pi^b, \{a,b\} \in \{+-, 00-+\}$ for different bins in W. $I = 0$ (solid black), narrow $I = 1$ (dotted black) and wide $I = 1$ (dashed black). Background dashed. [Moriya, Schumacher, Adhikari et al. 2013]

1. Experimental setup

2. Line-shape measurement

3. Spin-parity measurement

4. Conclusion

Theoretical basics I

The $\Lambda(1405)$ is so far (mostly) assumed to have $J^P = \frac{1}{2}^-$, but this has not been determined experimentally

Measuring spin

- consider the strong decay $Y^* \to Y\pi$, with J^P the spin and parity of Y^*
- the $Y\pi$ angular distribution will only depend on J

$$I(\theta_Y) = \text{const.} \qquad J = 1/2$$

$$I(\theta_Y) \propto 1 + \frac{3(1-2p)}{2p+1}\cos^2\theta_Y \qquad J = 3/2,$$

where θ_Y is the polar angle of the decay direction of Y in the Y^* rest frame, p describes the fraction of spin projections along the z axis

- uniform decay pattern is best evidence for spin $J = 1/2$

[Moriya, Schumacher, Aghasyan et al. 2014]

Measurements and analysis I

Analysis procedure

- plot the angular distribution of the projections $\cos\theta_\Sigma$ for each bin
- test each spin hypothesis using Monte-Carlo maximum likelihood fits, which employ angular decay probability distributions according to each hypothesis for $\Sigma\pi$
- compare each hypothesis by calculating a χ^2 probability

Meausrements and analysis I

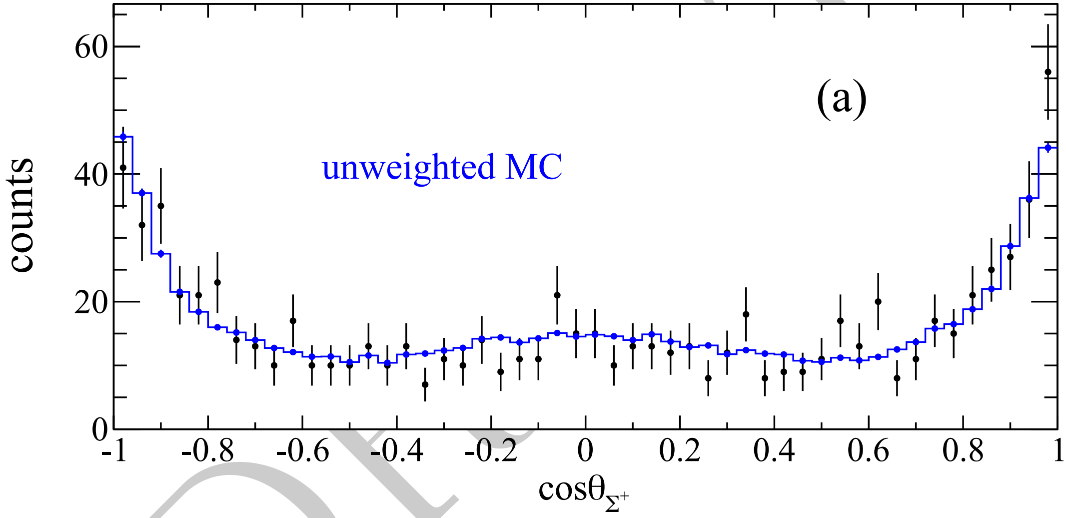

Figure 2: Distribution of decay angle of the σ^+ with Monte-Carlo fit using flat templates [Moriya, Schumacher, Aghasyan et al. 2014]

Theoretical basics II

Measuring parity

- the key to accessing the parity lies in determining the Polarization transfer to the decay product Y which we will denote $\mathbf{Q}$
- the angular distribution of $\mathbf{Q}$ will only depend on $\mathbf{P}$

$$\mathbf{Q}(\theta_Y) = \text{const.} \qquad J^P = 1/2^-$$

$$\mathbf{Q}(\theta_Y) = -\mathbf{P} + 2(\mathbf{P}\cdot\mathbf{q})\mathbf{q} \qquad J^P = 1/2^+$$

- $\mathbf{Q}$ can be measured from weak decay angular distribution of Y

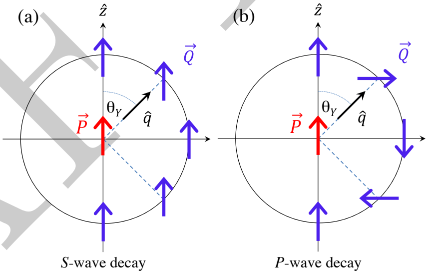

Polarization transfer in the strong decay $Y^* \to Y\pi$, [Moriya, Schumacher, Aghasyan et al. 2014]

[Moriya, Schumacher, Aghasyan et al. 2014 and Ref. therein]

Measurements and analysis II

Analysis procedure

- plot the angular distribution of the projections $\cos\theta_p$ for each bin
- determine the polarization using Monte-Carlo fits
- determine $Q_z(\cos\theta_{\Sigma^+})$ to get the parity (const. for $P = -$ quadratic for $P = +$)

Result: data is consistent with $J^P = 1/2^-$ but does in principle not rule out $J^P = 3/2^+$. $1/2^+$ and $3/2^-$ hypotheses can be discarded.

Measurements and analysis II

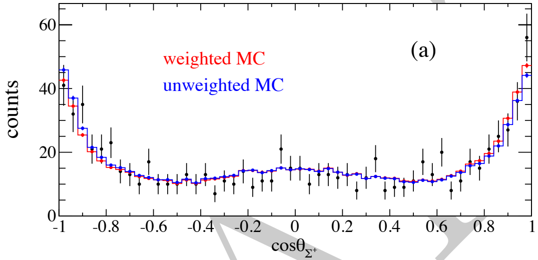

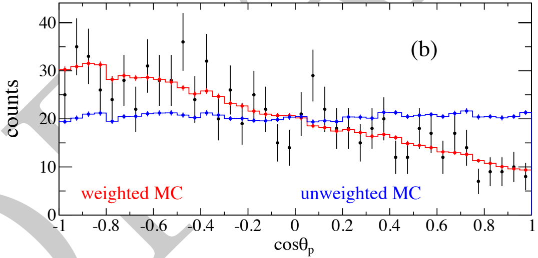

Distributions of the projections of (a)$\cos\theta_\Sigma$ and (b) $\cos\theta_p$ @ $2.65 < W < 2.75$ GeV and $0.70 < \cos\theta < 0.80$, [Moriya, Schumacher, Aghasyan et al. 2014]

Measurements and analysis II

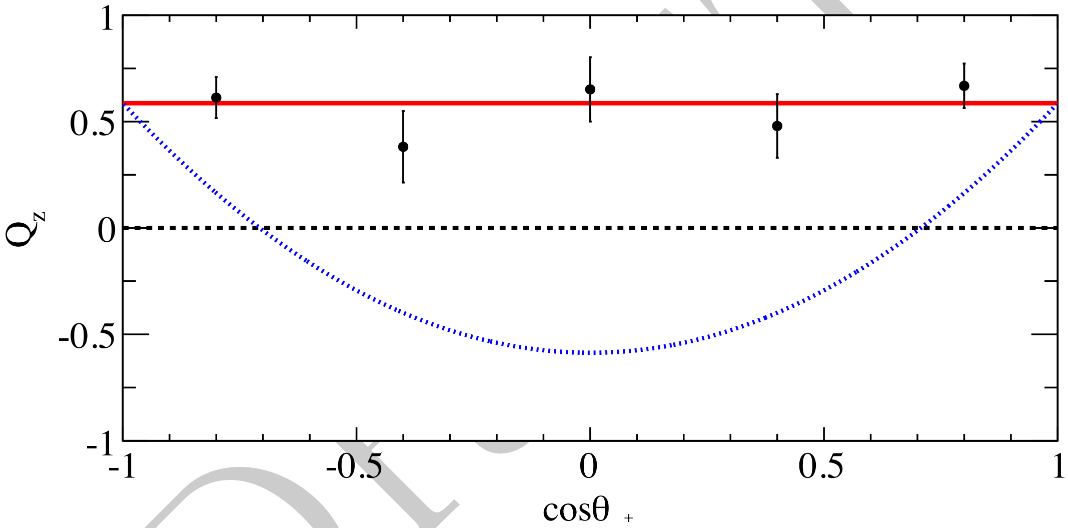

Angular distribution of the polarization Q_z @ $2.65 < W < 2.75\,\mathrm{GeV}$ and $0.70 < \cos\theta < 0.80$. Red: average, blue: expectation for P-wave decay. [Moriya, Schumacher, Aghasyan et al. 2014]

1. Experimental setup

2. Line-shape measurement

3. Spin-parity measurement

4. Conclusion

Conclusion

Lineshape measurement

- the CLAS detector was used to study $\gamma p \to K^+\Lambda(1405)$
- after selecting the correct events the true lineshape was extracted using Monte-Carlo sim. of the yield of other resonances
- the lineshapes in different decay channels differ from each other and from a simple Breit-Wigner
- a phenomenological isospin decomposition model was able to describe the data

Spin parity measurement

- the angular distribution of the decay $\Lambda(1405) \to \Sigma^+\pi^-$ was studied
- the angular distributions were tested against various J^P hypotheses
- the data is consistent with $J^P = 1/2^-$ but does not exclude $J^P = 3/2^+$

References

Flatté, S.M. (1976). 'Coupled-channel analysis of the $\pi\eta$ and $K\overline{K}$ systems near $K\overline{K}$ threshold'. In: *Physics Letters B* 63.2, pp. 224–227. ISSN: 0370-2693. DOI: https://doi.org/10.1016/0370-2693(76)90654-7. URL: https://www.sciencedirect.com/science/article/pii/0370269376906547.

Mecking, B.A. et al. (2003). 'The CEBAF large acceptance spectrometer (CLAS)'. In: *Nuclear Instruments and Methods in Physics Research Section A: Accelerators, Spectrometers, Detectors and Associated Equipment* 503.3, pp. 513–553. ISSN: 0168-9002. DOI: https://doi.org/10.1016/S0168-9002(03)01001-5. URL: https://www.sciencedirect.com/science/article/pii/S0168900203010015.

Moriya, K., R. A. Schumacher, K. P. Adhikari et al. (Mar. 2013). 'Measurement of the $\Sigma\pi$ photoproduction line shapes near the $\Lambda(1405)$'. In: *Phys. Rev. C* 87 (3), p. 035206. DOI: 10.1103/PhysRevC.87.035206. URL: https://link.aps.org/doi/10.1103/PhysRevC.87.035206.

Moriya, K., R. A. Schumacher, M. Aghasyan et al. (Feb. 2014). 'Spin and parity measurement of the $\Lambda(1405)$ baryon'. In: *Phys. Rev. Lett.* 112 (8), p. 082004. DOI: 10.1103/PhysRevLett.112.082004. URL: https://link.aps.org/doi/10.1103/PhysRevLett.112.082004.

Back-up: Continuous Electron Beam Accelerator Facility (CEBAF)

How can we access $\Lambda(1405)$ with this setup?

- employ radiator target for the electrons
- generate high energy photons using the *bremsstrahlung* process
- shoot high energy photons on proton target (LH2)
- then we can observe $\gamma p \to K^+\Lambda(1405)$ while knowing p_γ, p_p

Back-up: Spin-Parity – Measurements and analysis

Event selection

- select kinematic region where the $\Sigma\pi$ invariant mass is dominated by the $\Lambda(1405) \to M_{\Sigma\pi} \in$ 1.30 GeV to 1.45 GeV
- inspect nine bins in energy and angle, namely with CM energy at 2.6, 2.7 and 2.8 GeV and the three forwardmost kaon angle bins each

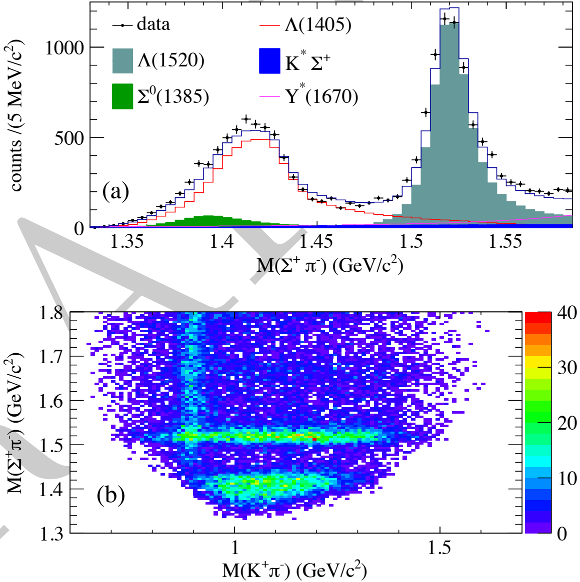

$\Sigma\pi$ and $K\pi$ invariant mass in the vicinity of the $\Lambda(1405)$, [Moriya, Schumacher, Aghasyan et al. 2014]